HHS Public Access

Author manuscript

J Pept Sci. Author manuscript; available in PMC 2020 April 01.

Published in final edited form as:

J Pept Sci. 2019 April ; 25(4): e3155. doi:10.1002/psc.3155.

Pharmacokinetic Stability of Macrocyclic Peptide Triazole HIV-1 Inactivators Alone and in Liposomes

Rachna Aneja[1,*], **Antonella Grigoletto**[2,*], **Aakansha Nangarlia**[1,3,*], **Adel A. Rashad**[1], **Steven Wrenn**[4], **Jeffrey M. Jacobson**[5], **Gianfranco Pasut**[2], and **Irwin Chaiken**[1]

[1]Department of Biochemistry and Molecular Biology, Drexel University College of Medicine, 245N 15th St, Philadelphia, PA 19102.

[2]Department of Pharmaceutical and Pharmacological Sciences, University of Padua, via Marzolo 5, Padua 35131, Italy

[3]School of Biomedical Engineering, Science and Health Systems, Drexel University, 3141 Chestnut Street, Philadelphia, PA 19104

[4]Department of Chemical and Biological Engineering, Drexel University, Philadelphia, PA 19104.

[5]Departments of Medicine and Neuroscience and Center of Translational AIDS Research, Lewis Katz School of Medicine, Temple University, Philadelphia, PA 19140.

Abstract

Previously, we reported the discovery of macrocyclic peptide triazoles (cPTs) that bind to HIV-1 Env gp120, inhibit virus cell infection with nanomolar potencies and cause irreversible virion inactivation. Given the appealing virus-killing activity of cPTs and resistance to protease cleavage observed *in vitro*, we here investigated *in vivo* pharmacokinetics of the cPT AAR029b. AAR029b was investigated both alone and encapsulated in a PEGylated liposome formulation that was designed to slowly release inhibitor. Pharmacokinetic analysis in rats showed that the half-life of FITC-AAR029b was substantial both alone and liposome-encapsulated, 2.92 and 8.87 h, respectively. Importantly, liposome-encapsulated FITC-AAR029b exhibited a 15-fold reduced clearance rate from serum compared to the free FITC-cPT. This work thus demonstrated both the *in vivo* stability of cPT alone and the extent of pharmacokinetic enhancement *via* liposome encapsulation. The results obtained open the way to further develop cPTs as long-acting HIV-1 inactivators against HIV-1 infection.

Introduction

With approximately 33.4 million adults living with HIV-1 worldwide, this infection remains one of the most significant global threats to public health. Although antiretroviral therapy (ART) has transformed HIV infection to a chronically managed disease, there is still a need to identify new strategies to treat and eventually eradicate established infection, including long-acting formulations (1–5).

Correspondence to: Irwin Chaiken.

*These authors contributed equally

Previously, we developed a peptide triazole (PT) class of HIV-1 inhibitors that target the viral gp120 protein on the HIV-1 virion surface and block both CD4 and co-receptor (CCR5/CXCR4) binding sites (6, 7). The PT class is highly active against both R5-and X4-tropic viruses and exhibits remarkable breadth amongst different HIV-1 subgroups (8). Interaction of PTs with HIV-1 Env causes gp120 shedding and consequent irreversible inactivation of free virus before host cell encounter (9). In addition, a subclass of PTs, with a free Cys residue at the C terminus of PT and denoted peptide triazole thiols (PTTs), causes virus membrane lysis and release of luminal capsid protein p24 (9). More recently, small potent cyclic PTs (cPTs) were identified (10, 11) that hold great potential as anti-HIV-1 therapeutic leads. The added value of cPTs over linear PTs is that they are more resistant to proteolytic degradation while retaining high affinity and specificity for interaction with target envelope HIV-1 glycoprotein gp120, and at the same time exhibiting no cellular toxicity.

In spite of the enticing virus inactivation and metabolic stability properties, the therapeutic potential of cPTs, as other small molecule leads, could potentially be limited by properties such as poor *in vivo* distribution and fast renal clearance resulting in low bioavailability. In the present study, we investigated the *in vitro* serum stability as well as the pharmacokinetic behavior of cPT alone and in a liposomal formulation. We considered the recent usage (12–15) of liposomal drug delivery systems to overcome bioavailability limitations, increase efficacy, prolong activity and reduce systemic toxicity of encapsulated agents. In the HIV-1/AIDS field, anti-HIV lipid nanoparticles containing a cocktail of lopinavir, ritonavir and tenofovir were shown to enhance plasma and intracellular drug levels in blood by several days, *versus* those of the corresponding non-encapsulated drugs (16). Here, we compared the serum *in vitro* stability of the cPT HIV-1 inactivator AAR029b (10), the fluorescein-labeled AAR029b (FITC-AAR029b), and a linear PT UM15 (Figure 1). We also investigated the potential to encapsulate AAR029b in liposomes coated with polyethylene glycol (PEG). In pharmacokinetic analysis in rats, we found that FITC-AAR029b exhibited a promising half-life ($T_{1/2}$) demonstrating good *in vivo* stability. The liposomal AAR029b had the advantage of slower clearance rate (Cl), a higher total drug exposure over time (AUC) and, pleasingly, increased serum half-life. The results of this work provide a first step in developing the proteolytically stable cPT for potential HIV-1 therapeutics.

Results

Synthesis of AAR029b and FITC-AAR029b

As shown in Figure 2, cyclic peptide triazole synthesis was performed on a solid phase resin using a previously described protocol (10). After cleavage and reverse-phase HPLC purification, the N-terminal AAR029b was reacted with FITC in DMF at room temperature to yield the FITC-AAR029b that was purified using reverse-phase HPLC. The N-terminal was chosen for labeling based on previous observations (10, 11) which showed the solvent exposure of the N-terminus.

Functional and stability properties of AAR029b and FITC-AAR029b

In order to assess the *in vivo* pharmacokinetic properties of macrocyclic peptide and its formulation, we synthesized an N-terminal labeled AAR029b derivative by using fluorescein

isothiocynate (FITC) as described in Experimental (see Figure 1 for chemical structures). The HPLC chromatogram demonstrating homogeneity and mass spectrum of purified FITC conjugated AAR029b are shown in Figure S1 and S2, respectively. The FITC-AAR029b was also found to be similarly active to AAR029b in both competition SPR gp120 interaction analysis and inhibition of cell infection with HIV-1 Bal.01 pseudo typed virus, as shown in Figure 3 and Table 1. Retention of function of FITC-AAR029b set the stage for using this molecule to encapsulate in liposomes for serum stability and pharmacokinetic studies.

Physicochemical characterization of AAR029b loaded liposomes

We initially prepared two PEGylated liposome formulations to encapsulate the macrocyclic peptide triazole AAR029b. The difference in these formulations was the length of the hydrocarbon tail of one of its constituent phospholipids, which was either **[a]** 1,2-dipalmitoyl-*sn*-glycero-3-phosphatidylcholine (DPPC) or **[b]** 1,2-distearoyl-*sn*-glycero-3-phosphatidylcholine (DSPC). The lipid compositions of the two formulations were **[1]** DPPC:Chol:mPEG2000-DSPE and **[2]** DSPC:Chol:mPEG2000-DSPE, in both cases at the same molar ratio of 2:1:0.5. The main objective was to compare the encapsulation efficiency and sustained release of AAR029b with variation of carbon chain length in DPPC and DSPC, 16- and 18-carbon length, respectively. The observed encapsulation efficiency for AAR029b was in the range of 55–60% for both formulations. The two liposomal formulations showed comparable AAR029b concentrations, of the order of 400 μM, after extrusion and purification to remove non-encapsulated AAR029b by gel filtration chromatography. The liposome sizes, determined by a Delsa™ Nano C particle analyzer, were in the range of approximately 150 nm. The compositions and size distributions of the two liposomal formulations are given in Table 2. Of note, both AAR029b liposome formulations were found to be stable at 4°C over a period of one month as demonstrated by retention of vesicle size and AAR029b content measured by light scattering and ultraviolet absorbance, respectively.

In vitro release kinetics and HIV-1 infection inhibition efficacies of AAR029b and its liposome formulations

The time dependence of release of macrocyclic AAR029b peptide from liposome formulations was monitored under physiological temperature conditions (Experimental). As shown in Figure 4, the DSPC:Chol:mPEG2000-DSPE formulation exhibited a slower release of AAR029b compared to the DPPC:Cholesterol:mPEG2000-DSPE formulation; ~ 60% and ~ 40% of AAR029b was retained in DSPC and DPPC liposomes after 96 h, respectively. There was no appreciable change in the size of the liposomal formulations after 96 h of AAR029b release. In addition, using virus infection inhibition assays, the antiviral activity of both formulations of liposomal AAR029b was shown to be retained even after the 96-hour/37 °C release experiment (see below). The slower and more sustained release of AAR029b at physiological temperature conditions from the liposomal formulation composed of DSPC phospholipid was attributed to its higher thermal stability due to the content of the 18-carbon acyl chain length component.

To assess the anti-HIV activity of AAR029b encapsulated in liposomal formulations, the recombinant single-round infection inhibition assay was performed with a panel of

pseudotyped viruses with HIV-1 Env from subtype B, namely BaL.01, YU-2 and JRFL. The results, shown in Table 3 and Figure 5A, demonstrate that AAR029b in the liposomal formulations inhibited infection by all three of the above-mentioned subtype B viruses with potencies comparable to those of non-encapsulated AAR029b. Furthermore, AAR029b and its liposome formulations did not inhibit viruses pseudotyped with a negative control envelope from vesicular stomatitis virus glycoprotein, VSV-G (data not shown), indicating that the inhibitory activities observed were specific to the HIV-1 envelope. No toxicity was observed for either the two formulations or the free AAR029b peptide in target HOS.CD4.CCR5 cells under the conditions used to determine infection inhibition potency at concentrations that were 50 fold higher than IC_{50} values after 24 hours continuous cellular exposure (Figure 5B).

In vitro serum stability of the AAR029b-liposome formulation

Previously, we found that AAR029b was resistant to proteolysis by the intestinal proteolytic enzymes trypsin and chymotrypsin (10). Here, to confirm systemic stability needed for pharmacokinetic analysis, we compared the effects of an *in vitro* human serum protease preparation on the 6-residue linear peptide triazole UM15 (see Figure 1 for chemical structure) (7), macrocyclic AAR029b, the DSPC:Chol:mPEG2000-DSPE formulation of AAR029b and FITC-AAR029b. As shown in Figure 6A and B, AAR029b, FITC-AAR029b and AAR029b in the liposome formulation all were intact after a 24 h treatment with a human serum protease mixture. (Figure S3 shows mass spectra for serum protease treated FITC-AAR029b at different time points up to 24h). In contrast, UM15 was rapidly degraded within a few minutes. These results demonstrate that both AAR029b and its FITC-conjugated counterpart retained metabolic stability in physiological assay conditions. The stability of FITC-AAR029b set the stage for using this fluorescently labeled cPT to track the *in vivo* PK properties of cPTs.

Pharmacokinetic analysis with FITC-AAR029b alone and encapsulated in DSPC:Chol:mPEG2000-DSPE liposomes

Since the DSPC:Chol:mPEG2000-DSPE formulation was shown to release FITC-AAR029b at a slower sustained rate *in vitro* compared to DPPC:Chol:mPEG2000-DSPE formulation, we chose the former to perform a pharmacokinetic analysis in rats. FITC-AAR029b and its liposomal formulation were compared for residence time in blood samples collected at different time points after tail vein administration. As shown in Figure 7, the plasma level of free FITC-AAR029b, determined by fluorescence measurements (λex =494nm, λem =520 nm), decreased more rapidly and was not detectable beyond 7 hours. In contrast, the liposome formulation showed a marked half-life prolongation of FITC-AAR029b, with detectable levels of peptide for over 24 hours. The pharmacokinetic parameters are reported in Table 4 for FITC-AAR029b and the liposomal formulation. The half-life of FITC-AAR029b was increased 3.5-fold as a result of incorporation into DSPC:Chol:mPEG2000-DSPE liposomes. In addition, the clearance rate and the apparent volume of distribution of the liposomal formulation were significantly reduced compared to the free cPT. The parameter AUC, the Area Under the Curve, reflecting the FITC-AAR029b exposure in blood per unit time, was increased 15-fold compared to non-encapsulated FITC-AAR029b.

Confirmation of *in-vivo* structural integrity of FITC-AAR029b

We sought to confirm that the PK parameters derived from fluorescence measurements were directly correlated to intact FITC-AAR029b and not due to free FITC or FITC-peptide fragments derived by FITC-AAR029b metabolic breakdown in blood. Integrity of FITC-AAR029b released from liposomes was investigated in selected pharmacokinetic samples that were analyzed by UPLC-Q-TOF mass spectrometry. In particular, for two rats, 15 min and 3 h time points were selected based on the estimation of their peptide content *vs* the limit of detection of the instrument. Expected amounts of FITC-AAR029b in these samples were as follows: 1) for rat #1, 4.57 ng and 2.9 ng at 15 min and 3 h, respectively, and 2) for rat #3, 4.28 ng and 2.6 ng at 15 min and 3 h, respectively. All of these values were above the limit of detection of the instrument. The mass spectrum of FITC-AAR029b obtained by direct infusion revealed two signals, one corresponding to a single charged FITC-AAR029b with an m/z ratio of 1393.45, and the second corresponding to the double charged FITC-AAR029b with an m/z ratio of 697.23 (Figure S4). The TIC (Total Ion Current) chromatograms and mass spectrometry data of liposomal FITC-AAR029b at the selected time points were compared to the references (plasma without the liposomal formulation and FITC-AAR029b liposome incubated in plasma) to identify FITC-AAR029b, after ion mass selection at 697.23 $[M+2H]^{2+}$, with a tolerance of 0.05. In the above analysis, the ion with m/z of 697.23 was selected for screening *in vivo* samples because it was found to be more abundant than the single charged species during development of the analytical method. The time of elution of FITC-AAR029b in the TIC chromatogram was identified and confirmed between 9 to 11 min (Figure S5 and S6).

As shown in the TIC chromatographic profile of plasma alone (negative control sample), after deproteinization with ACN (Figure S7), more than one chromatographic peak was observed corresponding to the m/z of 697. However, upon analyzing the mass spectra for plasma alone, no ion was found corresponding to FITC-AAR029b (Figure S8) in the 9 to 11 min time frame. This observation confirmed that the 696–699 m/z mass region could unequivocally be used for determination of FITC-AAR029b.

The focused mass spectra of isotope distribution for the cases of the liposomal FITC-AAR029b plasma time points at 15 min and 3 h of rat #3 are reported in Figure 8. The TIC chromatograms and the entire mass spectra of the same plasma time points are reported in Figures S9, S10, S11 and S12. The intactness of the labeled peptide released from liposome was observed until 3h of circulating time. From this study and the above investigation of stability of FITC-AAR029b in serum, we can conclude that the concentrations of pharmacokinetic samples, detected through the fluorescence of the linked dye to AAR029b, corresponded to the intact peptide conjugated to the fluorescein.

Discussion

We previously found that cyclizing linear peptide triazoles targeting HIV-1 Env gp120 led to a cPT molecular class that retained high potency in irreversibly inactivating HIV-1 and at the same time were stable against model proteases *in vitro* (10). This suggested the potential use of cPTs as HIV-1 therapeutic leads and therefore, the central aim of the current work to evaluate their *in vivo* stability. For this purpose, we synthesized a fluorescein-labeled cPT

(FITC-AAR029b) and tested its pharmacokinetic behavior in rats, both alone and in liposomal formulations. The present proof of concept study involved intravenous administration of the cPT and its liposomal formulations. This was chosen because it is the most common and conventional mode to evaluate the fate of drug in the systemic circulation of small animals. Studies have shown that more equivalents of drug enter the circulation via intravenous compared to subcutaneous administration (17). The treatment of HIV infection warrants comparison of the efficacy and biodistribution of the formulations via different modes of administration, the intravenous mode initially, but ultimately the more clinically convenient subcutaneous mode of delivery (18). Here, we found that FITC-AAR029b alone had a promising *in vivo* half-life, confirming the previous *in vitro* results (10). At the same time, liposome encapsulation both improved half-life and greatly reduced the clearance rate of the FITC-AAR029b. These observations confirmed the cPT stability against serum proteases *in vivo*.

An important outcome of the current investigation was the finding of encouraging pharmacokinetic properties for the cPT alone. The half-life of the FITC-AAR029b was 2.92 h, a striking improvement over the half-life of 16–23 minutes observed for linear peptide triazole derivatives in an earlier preliminary experiment (data not shown). The half-life of this cPT was even greater than the half-life of 1.57 h reported for the clinically approved HIV-1 fusion inhibitor Enfurvitide or T-20 (19). Furthermore, the pharmacokinetic properties of FITC-AAR029b were similar to those of a known small molecule HIV-1 entry inhibitor, BMS-378806, and in fact the clearance rate in rats of the free FITC-AAR029b, 136 mL/h, was much slower than that reported for BMS-378806, ~ 1800mL/h (20).

The current study also showed that enhancing the PK parameters of cPTs is possible through liposomal formulations. We were able to achieve a high, 50–55%, cPT-loading efficiency into liposomes. The observed water solubility and the hydrophilic nature of AAR029b (cLogP value of 0.36 as calculated using Chemdraw Version, 15.0.0106) make it likely that the loaded cPT resided in the hydrophilic core of the lipid vesicle (21). The liposomes were designed using phospholipids that undergo phase transition above 37 °C and thus are relatively stable at physiological temperature (22). The PEG moiety was incorporated in the formulations to further stabilize the liposomes and ultimately increase the residence time of cPT in the circulation. Importantly, we found that the DSPC:Chol:mPEG2000-DSPE formulation of FITC-AAR029b was stable in plasma and that the liposomes had a 15-fold reduced systemic clearance rate compared to the free FITC-AAR029b. The slower release from the liposome formulations also protected FITC-AAR029b from elimination, after intravenous administration in rats, as indicated by the prolonged half-life (9h *vs* ~ 3h for the free FITC-AAR029b). The work conducted here has provided evidence that liposomal formulations can be used as a delivery mechanism for the potent cPTs. Further *in vivo* PK studies are anticipated, ultimately in multiple animal models, in order to help define cPT and liposomal-cPT dosing for antiviral efficacy trials.

The liposomal formulation results of this work both reflect and extend the potential of liposomes for drug delivery generally and for delivery to mucosal sites of HIV-1 proliferation in particular. Longer systemic residence time using liposome drug formulations has been reported (12, 23–25). Even though HAART has been dramatically successful in

suppressing HIV-1 viral replication, latent infection persists in the lymphoid tissues and other anatomical and cellular reservoirs (26). Sub-optimal drug concentrations in tissues devoid of blood supply or with an anatomical barrier (27, 28) have been found to permit continued HIV-1 production. To find a cure for AIDS, barriers to established reservoirs need to be overcome (2, 5, 29). Several studies with surface-modified liposomal nanocarriers for intracellular delivery of anti HIV-1 drugs have been encouraging in enabling access to lymphoid tissues (30, 31). Given the precedent for targeting latent reservoirs utilizing liposome technology (16, 32), the results reported here open up the possibility to test the unique anti-Env cPT loaded in liposomes against latently HIV-1 infected cells.

Findings emerging from this study encourage further investigations of both HIV-1 inactivating cPT synthetic designs with increasing metabolic stability and their liposomal delivery. The metabolic stability and significant half-life properties of AAR029b alone provide a useful starting point; and, as shown here, liposomal encapsulation can significantly improve the PK properties of this class of inhibitors. Cyclic PTs and their liposome formulations are not envisioned to replace current HAART components but instead to introduce agents with an entirely new mode of therapeutic action. Long-acting treatments may also be useful as a part of a “treatment as prevention” or pre-exposure prophylaxis (PrEP) strategy.

Experimental

Materials

HOS cells expressing CD4/CCR5 were acquired from the NIH AIDS Reagent Program from Dr. Nathaniel Landau. DNA sequences encoding BaL.01 Env and NL4–3R$^-$ Env$^-$Luc$^+$ core were obtained from the NIH AIDS Reagent Program from Dr. John Mascola and Dr. Nathaniel Landau, respectively. The plasmid encoding JR-FL gp160 and YU-2 gp160 was a kind gift of Drs. Alon Herschhorn and Joseph Sodroski. The lipids DSPC (1,2-distearoyl-*sn*-glycero-3-phosphocholine), DPPC (1,2-dipalmitoyl-*sn*-glycero-3-phosphocholine) and maleimide-PEG2000-DSPE (1,2-distearoyl-*sn*-glycero-3-phosphoethanolamine-N-[maleimide(polyethylene glycol)-2000]) were obtained from Avanti Polar Lipids, Inc. and Cholesterol from Sigma, Inc.

Macrocyclic peptide synthesis

The macrocyclic peptide AAR029b was synthesized as described previously (10). Briefly, after peptide sequence assembly using (DIC/Oxyma activation scheme) microwave synthesizer (CEM LibertyBlue™), the N-terminal Asp side chain carboxyl group was deprotected by 20% piperidine in DMF during the final microwave deprotection step. The peptide-bound resin was then subjected to selective deprotection conditions (2% hydrazine in DMF, 3 × 40 mL ×10 min) to deprotect the Lys side chain NH_2 protecting group. Complete isopeptide bond formation for cyclization was achieved using two microwave coupling steps. On-resin click reaction with the ethynylferrocene was achieved by shaking the peptide-bound-resin in a mixture of acetonitrile, water, DIEA and pyridine for 12 h at room temperature in the presence of catalytic CuI. Acidic deprotection/cleavage using TFA/TIS/water yielded the crude peptides. Purification (to ≥ 95% homogeneity) from the

soluble crude peptide was achieved using a C18 RP-HPLC preparative column (ACN/H_2O/0.1% TFA), and the product was freeze dried. Purity check of the macrocycle was carried out using analytical C18 RP-HPLC. Chemical structure validation of the macrocycle was carried out using matrix-assisted laser desorption ionization time-of flight mass spectrometry (MALDI-TOF MS).

FITC-labeling of macrocyclic AAR029b

Macrocyclic peptide AAR029b (1 eq) and FITC (1 eq) were dissolved in DMF, and a catalytic amount (a few drops) of TEA was added. The reaction was stirred, in the dark, for 24 hours at 4 °C. The FITC-AAR029b conjugate product was directly purified from unreacted FITC by RP-HPLC, lyophilized and the collected products were analyzed by ESI-TOF mass spectrometry. The conjugation of FITC to AAR029b was also confirmed by UV-Vis absorption ($\boldsymbol{\varepsilon}$ =176.15, $\boldsymbol{\lambda}$ =494 nm) in PBS, pH 7.4.

Protein reagents

Soluble CD4 (sCD4) was produced and purified as described before (7). Monoclonal antibody 17b was obtained from Strategic BioSolutions. Wild-type (WT) HIV-1 $gp120_{YU-2}$ was produced from a pcDNA3.1 vector encoding a V5 sequence tag (GKPIPNPLLGLDST) inserted N-terminal to the C-terminal His6 tag. The vector also carried the mammalian codon-optimized sequence for a CM5 secretion peptide and $gp120_{YU-2}$ (a gift from Drs. Navid Madani and Joseph Sodroski). DNA for transient transfection was purified using a Qiagen MaxiPrep kit (Qiagen) and transfected into HEK 293F cells according to the manufacturer's protocol (Invitrogen). Five days after transfection was initiated, cells were harvested and spun down, and the supernatant was filtered through a 0.2 μm filter (Corning). Purification was performed over a 17b antibody-coupled column prepared using NHS-activated Sepharose (GE Healthcare). The gp120 was eluted from the column using 0.1 M Glycine buffer pH 2.4 and diluted immediately into 1 M Tris pH 8.0. Protein identity in the eluted fractions was confirmed by SDS-PAGE and western blotting using antibody D7324 (Aalto Bioreagents). After pooling the peak fractions, additional purification including removal of aggregates was performed with a pre-packed Superdex 200 HR gel filtration chromatography column (GE Healthcare). Monomer-containing fractions were identified by SDS-PAGE/Western blotting with mAb D7324, pooled, concentrated, frozen and stored at −80 °C.

Surface plasmon resonance (SPR) assays

Binding activity of the FITC-AAR029b to gp120 was assessed by an SPR competition assay. SPR experiments were performed on a Biacore 3000™ optical biosensor (GE Healthcare). All experiments were carried out at 25 °C using standard PBS buffer pH 7.4 with 0.005% surfactant Tween. A CM5 sensor chip™ was derivatized by standard 1-ethyl-3-(3-dimethylaminopropyl) carbodiimide (EDC)/N-hydroxysuccinimide (NHS) chemistry, and coupling was achieved through ligand amine groups. Antibody 2B6R (α-human IL5R) was immobilized for use as a control surface. For competition experiments, soluble four domain CD4 and 17b antibody were immobilized on separate chip surfaces through standard EDC/NHS chemistry (above). Serial dilutions of FITC–AAR029b were mixed with

monomeric wt $gp120_{YU-2}$ and binding of gp120 to chip-immobilized sCD4 and 17b measured by SPR response. Mean inhibitory concentrations (IC_{50}) were calculated after fitting the data to a logistic function (Origin Lab).

For kinetic analyses, typically 2000–3000 RUs of protein reagents were immobilized on SPR chips, and analytes were passed over the surface at 50–100 μL/min. Surface regeneration was achieved by a 5 μL injection of 10 mM HCl solution at 100 μL/min. Analysis of peptide-mediated sCD4 and mAb 17b inhibition was achieved by injecting a fixed concentration of HIV-1 $gp120_{YU-2}$ (250 nM), with increasing peptide concentrations, over sCD4 (2000 RU) and mAb 17b (1000 RU) surfaces for 5 minute association and 5 minute dissociation at a flow rate of 50 μL/min in PBS. Regeneration of the surface was achieved by a single 10 second pulse of 1.3 M NaCl/35 mM NaOH and a single 5-second pulse of 10 mM glycine, pH 1.5, for sCD4 and mAb 17b, respectively. All analyses were performed in triplicate. Data analysis was performed using BIAEvaluation v4.0 software (GE Healthcare). Signals from buffer injection and control surface binding were subtracted in all experiments to account for nonspecific binding.

For kinetic parameter determination, we used a method similar to that used by Morton et al. (33). The signal from the highest concentration of the analyte was used to calculate the off rate (kd) using a simple 1:1 binding model. For each concentration, the association phase data were fitted to a simple 1:1 bimolecular interaction model using the BIAEvaluation software. The resulting Req values were used to fit the corresponding steady state model and calculate equilibrium dissociation constant (K_D) values. The evaluation method for SPR inhibition data included a calculation of the inhibitor concentration at 50% of the maximal response (IC_{50}). The inhibition curve was converted into a calibration curve by the use of a fitting function. The fitting was done using the 4-parameter equation in BIAevaluation software,

$$\text{Response} = R_{\text{high}} - \frac{\left(R_{high} - R_{low}\right)}{1 + \left(\frac{\text{Conc}}{\text{A}_1}\right)^{\text{A}_2}},$$

where R_{high} is the response value at high inhibitor concentrations and R_{low} is response at low inhibitor concentrations. Conc. is the concentration of inhibitor, and A_1 and A_2 are fitting parameters. At the IC_{50} the following is true:

$$\text{Response} = R_{\text{high}} - \frac{\left(R_{high} - R_{low}\right)}{2}.$$

Under this condition, A_1 = Conc and is therefore taken as the desired IC_{50} parameter.

Preparation of macrocyclic peptide AAR029b/FITC-AAR029b loaded liposomes

Lipid composition for the PEGylated liposomes was a) DPPC:Chol:mPEG2000-DSPE, and b) DSPC:Chol:mPEG2000-DSPE, in both cases at a molar ratio of 2:1:0.5. DPPC is 1,2-

dipalmitoyl-*sn*-glycero-3-phosphatidylcholine; DSPC is 1,2-distearoyl-*sn*-glycero-3-phosphatidylcholine; DSPE is 1,2-distearoyl-*sn*-glycero-3-phosphoethanolamine-N-[methoxy(PEG)-2000]. The lipids were mixed in a round bottom flask in 2 ml of chloroform and then evaporated using Rotavapor®. The lipid film was further dried under vacuum overnight and hydrated with 1ml of PBS buffer pH 7.4. The liposomes were then loaded with either AAR029b or FITC-AAR029b. The resulting suspensions were subjected to 10 cycles of freezing and thawing, then extruded 21 times through a stainless-steel extrusion device using two stacked polycarbonate filters with 400 nm, 200 nm and 100 nm pore size. The non-encapsulated AAR029b (or FITC-AAR029b) was separated from encapsulated AAR029b by gel filtration chromatography using HiPrep 26/10 Desalting Sephadex G-25 Fine, cross-linked dextran.

Size measurement and determination of encapsulation efficiency

The size of the liposomes was measured using dynamic light scattering. Mean size, size distribution and zeta potential were evaluated using a Beckman Coulter, Delsa™, Nano C particle analyzer. The encapsulation efficiency of AAR029b/FITC-AAR029b was measured by treating the AAR029b/FITC-AAR029b loaded lipid vesicles with 1:2 volumes of isopropyl alcohol, and the lipid mass was isolated from the rest of the solution by centrifugation at 13000 rpm for 30 min. The supernatant was then measured for the AAR029b and FITC-AAR029b content using absorbance at 280 nm (for AAR029b) and 280 nm and 490 nm (for FITC-AAR029b) respectively. cPT loading efficiency (%) was calculated using the following equation = (Amount of cPT retained/cPT taken initially) × 100.

In vitro release of macrocyclic peptide triazole from liposomes

Macrocyclic AAR029b loaded in two different liposome formulations was assayed for release kinetics using Slide-A-Lyzer mini dialysis devices. Briefly, 0.5 ml of the AAR029b loaded liposome suspension was taken into the dialysis device made of regenerated cellulose membrane (10 kDa Mol wt cut off). The device was then placed in a conical tube containing phosphate buffer saline (PBS), pH 7.4 at 37 °C under orbital shaking conditions at 50 rpm. Fresh PBS buffer was replenished every 24 h, and release kinetics was measured for 5 days. Aliquots of residual liposomal content retained in the dialysis device at different time points was lysed using 1:1 volume of isopropanol to calculate the amount of AAR029b retained in liposomes using absorbance at 280 nm. Aliquots were also withdrawn from the release medium (PBS buffer) at different time points and analyzed for the amount of released AAR029b macrocyclic molecule using absorbance at 280 nm. The dialysis buffer was completely exchanged with fresh PBS buffer after every 24 h and the released peptide was measured as described above. The release profile of AAR029b peptide from liposomes was monitored for 5 days. The experiment was repeated three times for two different formulations, namely a) DPPC:Chol:mPEG2000-DSPE and b) DSPC:Chol:mPEG2000-DSPE. The volume of liposomal formulation and size of the vesicle were recorded at the end of the release study to assess any dilution effect of liposomal formulation or size changes of the vesicles that occurred during drug release.

In vitro stability analyses of AAR029b and FITC-AAR029b to proteolysis in serum

Macrocyclic peptide AAR029b and its liposome formulations were subjected to temperature-equilibrated 25% human serum supplemented with RPMI nutrient media at 37 °C similarly as described before (34). The final concentration of cPT was 100 μg/ml for both incubations, the peptide alone and its liposome formulation. The initial time was recorded and, at different time intervals (from 0 to 16 h), a 100 μL aliquot of the reaction solution was removed and added to 200 μL of 6% aqueous trichloroacetic acid (TCA) to precipitate serum proteins. The cloudy reaction was cooled to 4 °C for 1 min and spun at 18,000 × g for 5 min to pellet the precipitate. The soluble fraction of the reaction mixture was examined by RP-HPLC on an analytical C18 column (ACN/H_2O/0.1% TFA) at a flow rate of 1 ml/min, with absorbance detected at 280 nm. For FITC-AAR029b *in vitro* stability analysis, samples from RP-HPLC were further evaluated in tandem by mass spectrometry (Waters QDa ESI detector®) to ensure retention of intactness as a prelude to *in vivo* pharmacokinetic analysis.

Ethical statement for *in vivo* experiments

The study protocol was approved by the Ethics Committee of the University of Padova and the Italian Ministry of Health (938/2016-PR), and animals were handled in compliance with national (Italian) Legislative Decree 116/92 guidelines and with the “Guide for the Care and Use of Laboratory Animals” by the National Research Council of the National Academies.

Pharmacokinetic analysis

Pharmacokinetic profiles of FITC-AAR029b and liposome encapsulated FITC-AAR029b were determined in Sprague-Dawley rats (200–250 g; 2 animals in two groups). Samples were diluted in saline buffer and 400 μL of each solution (containing a 3 μg dose of fluorescein equivalent) were administered *via* tail vein to rats anaesthetized with 5% isoflurane gas (mixed with O_2 in enclosed cages). At predetermined times, blood samples (150 μL) were withdrawn from the tail vein and centrifuged at 1,500 × g for 15 min. 50 μL of the supernatant (plasma) were diluted as needed with PBS and the fluorescence was determined (λex = 494 nm, λem = 520 nm). The equivalent peptide content was determined against a calibration curve of FITC-AAR029b and FITC-AAR029b liposomes. The experiment was performed in duplicate.

Estimation of structural integrity of FITC-AAR029B in plasma *in vivo*

From the previous pharmacokinetic experiments, selected plasma samples were analyzed by Q-TOF mass spectrometry to confirm that fluorescence measurements were directly correlated to intact FITC-AAR029b and not due to free FITC or FITC-peptide fragments after *in vivo* administration. The plasma samples were chosen based on their expected content of FITC-AAR029b calculated from the pharmacokinetic profile. Plasma samples from15 min and 3 h time-points of two different rats were treated with Triton X-100 resulting in a final concentration of 1% (v/v). To 50 μL of such a plasma solution, 350 μL of ACN was added to achieve protein precipitation. The samples were centrifuged at 20,000 × g for 5 min. The supernatants were collected and freeze-dried. Dried samples were dissolved in 10 μL of water/ACN 98:2 both with 0.1% of formic acid and analyzed by a UPLC-Q-TOF

mass spectrometry instrument (Waters Xevo G2-S QTof) with a Grace Vydac TP C18 column (150 × 1 mm; 5 μm), maintained at 32° C, flow-rate 0.1 mL/min, eluted with a solvent gradient of water/ACN both containing 0.1% formic acid. As references, a known amount of FITC-AAR029b liposome in plasma and a sample of plasma and PBS without the liposomal formulation were treated as reported above. Mass spectrometry data of liposomal FITC-AAR029b at the selected time points were compared to the references to identify FITC-AAR029b, after ion mass selection at 697.23, $[M+2H]^{2+}$, with a tolerance of 0.05. The value of 697.23 is the exact double charged mass of FITC-AAR029b, as identified by direct infusion in the mass spectrometer of the FITC-AAR029b.

HIV-1 pseudovirus production

Pseudoviruses were produced as described before (7, 35). Briefly, HEK 293T cells (3×10^6) were co-transfected with 4 μg of BaL.01 gp160 plasmid and 8 μg of NL4–3 R^- Env^- Luc^+ core DNA, using polyethyleneimine (PEI) as a transfection vehicle. YU2 and JRFL pseudoviruses were produced in an identical manner as BaL.01 pseudoviruses, except that the transfection reagent used in the latter case was Fugene. After 72 hours, the supernatant containing virus was collected and filtered using a 0.45 μm filter (Corning) before being purified *via* gradient centrifugation on a 6% - 20% iodixanol gradient (Optiprep, Sigma Aldrich) spun in an Sw41 Ti rotor (Beckman Coulter) at 110,000 × g for 2 hours at 4 °C. The bottom 5 ml were collected and diluted in serum free medium before being aliquoted and frozen at −80 °C. Importantly, viruses isolated by the iodixanol gradient method were found to contain no exosomes as judged by the absence of CD45 as described in (36). All batches of pseudovirus were titrated for infectivity and p24 content immediately after production.

Cell infection inhibition assay

Pseudoviral infection assays carried out as described previously (7, 35) were used to validate the viruses used in this work and to track the effects of both AAR029b and liposome formulations on infectivity. Briefly, HOS.T4.R5 cells were seeded the day before at 7,000 cells, 100 μl/well in 96 well plates. Virus stocks were diluted in growth media such that the final dilution gave 1×10^6 luminescence counts. Cells were seeded the day before at 7,000 cells, 100 μl/well in 96 well plates. When used, liposome dilutions were mixed with diluted virus (1:1, v/v) through inversions and incubated at 37 °C for 30 minutes. Controls were mixed with an equivalent amount of PBS and no liposomes. Medium was removed from the plates and virus-containing medium was added. The plates were incubated for 24 hours at 37 °C before the medium was changed. The medium was removed and the cells were lysed 48 hours after the virus was added to the plate, (Passive Lysis Buffer, Promega). The lysate was then transferred to a white well plate (Greiner) and mixed with 1 mM Luciferin salt (Anaspec) diluted in 0.1 M potassium phosphate buffer containing 0.1 M magnesium sulfate and the luminescence measured using a Wallac 1450 Microbeta Luminescence reader at 490 nm.

MTT assay for cell viability

The HOS.T4.R5 cells were cultured in the nutrient medium in a humidified atmosphere (37 °C and 5% of CO_2) at cell density 7,000 cells, 100 μl/well in 96 well plates a day before

the MTT assay. The cells were then treated with different dilutions of liposome formulations with or without encapsulated AAR029b, for 24 h along with a free non-encapsulated AAR029b control. Then, the culture medium containing liposome formulations/free AAR029b peptide were washed three times with PBS before being cultured in fresh medium for another 24 h. At the end of the incubation, 10 μl at 10 mg/ml of tetrazolium salt premix reagent WST-1 in PBS (TaKaRa Bio, Inc., manufacturer's protocol) was added to 100μl medium per well. Cell viability was determined using the formazan product measured using a microplate reader (Molecular Devices) at an absorbance wavelength of 450 nm.

Supplementary Material

Refer to Web version on PubMed Central for supplementary material.

Acknowledgements:

We thank the Drexel University Clinical Translational Research Institute, the Campbell Foundation, NIH P01 GM56550 and NIH R01 GM111029 for financial support of this work.

Abbreviations.

ACN	acetonitrile
ART	antiretroviral Therapy
AUC	the Area Under the Curve
Boc	Tertbutyloxycarbonyl
cPT	Cyclic Peptide Triazole
DIC	N,N′-Diisopropylcarbodiimide
DPPC	1,2-dipalmitoyl-*sn*-glycero-3-phosphatidylcholine
DSPC	1,2-distearoyl-*sn*-glycero-3-phosphatidylcholine
EDC	1-ethyl-(dimethylaminopropyl) carbodiimide
FITC	Fluorescein isothiocynate
MALDI-TOF MS	matrix-assisted laser desorption ionization time-of flight mass spectrometry
NHS	N-hydroxysuccinimide
PEG	polyethylene glycol
PTTs	peptide triazole thiols
PEI	polyethyleneimine
TCA	trichloroacetic acid
TIC	Total Ion Current

SPR	Surface Plasmon Resonance
UPLC	Ultra High Performance Liquid Chromatography

References

1. Margolis DM, Garcia JV, Hazuda DJ, Haynes BF. Latency reversal and viral clearance to cure HIV-1. Science. 2016;353(6297):aaf6517. [PubMed: 27463679]
2. Kimata JT, Rice AP, Wang J. Challenges and strategies for the eradication of the HIV reservoir. Curr Opin Immunol. 2016;42:65–70. [PubMed: 27288651]
3. Swindells S, Flexner C, Fletcher CV, Jacobson JM. The critical need for alternative antiretroviral formulations, and obstacles to their development. J Infect Dis. 2011;204(5):669–74. [PubMed: 21788451]
4. Siliciano RF. Opening Fronts in HIV Vaccine Development: Targeting reservoirs to clear and cure. Nat Med. 2014;20(5):480–1. [PubMed: 24804757]
5. Chun TW, Moir S, Fauci AS. HIV reservoirs as obstacles and opportunities for an HIV cure. Nat Immunol. 2015;16(6):584–9. [PubMed: 25990814]
6. Gopi H, Umashankara M, Pirrone V, LaLonde J, Madani N, Tuzer F, et al. Structural determinants for affinity enhancement of a dual antagonist peptide entry inhibitor of human immunodeficiency virus type-1. J Med Chem. 2008;51(9):2638–47. [PubMed: 18402432]
7. Umashankara M, McFadden K, Zentner I, Schon A, Rajagopal S, Tuzer F, et al. The active core in a triazole peptide dual-site antagonist of HIV-1 gp120. ChemMedChem. 2010;5(11):1871–9. [PubMed: 20677318]
8. McFadden K, Fletcher P, Rossi F, Kantharaju, Umashankara M, Pirrone V, et al. Antiviral breadth and combination potential of peptide triazole HIV-1 entry inhibitors. Antimicrob Agents Chemother. 2012;56(2):1073–80. [PubMed: 22083481]
9. Bastian AR, Kantharaju, McFadden K, Duffy C, Rajagopal S, Contarino MR, et al. Cell-free HIV-1 virucidal action by modified peptide triazole inhibitors of Env gp120. ChemMedChem. 2011;6(8): 1335–9, 18. [PubMed: 21714095]
10. Rashad AA, Kalyana Sundaram RV, Aneja R, Duffy C, Chaiken I. Macrocyclic Envelope Glycoprotein Antagonists that Irreversibly Inactivate HIV-1 before Host Cell Encounter. J Med Chem. 2015;58(18):7603–8. [PubMed: 26331669]
11. Rashad AA, Acharya K, Haftl A, Aneja R, Dick A, Holmes AP, et al. Chemical optimization of macrocyclic HIV-1 inactivators for improving potency and increasing the structural diversity at the triazole ring. Org Biomol Chem. 2017;15(37):7770–82. [PubMed: 28770939]
12. Immordino ML, Dosio F, Cattel L. Stealth liposomes: review of the basic science, rationale, and clinical applications, existing and potential. Int J Nanomedicine. 2006;1(3):297–315. [PubMed: 17717971]
13. Ramana LN, Sharma S, Sethuraman S, Ranga U, Krishnan UM. Stealth anti-CD4 conjugated immunoliposomes with dual antiretroviral drugs--modern Trojan horses to combat HIV. Eur J Pharm Biopharm. 2015;89:300–11. [PubMed: 25500283]
14. Allen TM, Cullis PR. Liposomal drug delivery systems: from concept to clinical applications. Adv Drug Deliv Rev. 2013;65(1):36–48. [PubMed: 23036225]
15. Sercombe L, Veerati T, Moheimani F, Wu SY, Sood AK, Hua S. Advances and Challenges of Liposome Assisted Drug Delivery. Front Pharmacol. 2015;6:286. [PubMed: 26648870]
16. Freeling JP, Koehn J, Shu C, Sun J, Ho RJ. Long-acting three-drug combination anti-HIV nanoparticles enhance drug exposure in primate plasma and cells within lymph nodes and blood. AIDS. 2014;28(17):2625–7. [PubMed: 25102089]
17. Wilson KD, Raney SG, Sekirov L, Chikh G, deJong SD, Cullis PR, et al. Effects of intravenous and subcutaneous administration on the pharmacokinetics, biodistribution, cellular uptake and immunostimulatory activity of CpG ODN encapsulated in liposomal nanoparticles. Int Immunopharmacol. 2007;7(8):1064–75. [PubMed: 17570323]

18. Jin JF, Zhu LL, Chen M, Xu HM, Wang HF, Feng XQ, et al. The optimal choice of medication administration route regarding intravenous, intramuscular, and subcutaneous injection. Patient Prefer Adherence. 2015;9:923–42. [PubMed: 26170642]
19. Zhu X, Zhu Y, Ye S, Wang Q, Xu W, Su S, et al. Improved Pharmacological and Structural Properties of HIV Fusion Inhibitor AP3 over Enfuvirtide: Highlighting Advantages of Artificial Peptide Strategy. Sci Rep. 2015;5:13028. [PubMed: 26286358]
20. Lin PF, Blair W, Wang T, Spicer T, Guo Q, Zhou N, et al. A small molecule HIV-1 inhibitor that targets the HIV-1 envelope and inhibits CD4 receptor binding. Proc Natl Acad Sci U S A. 2003;100(19):11013–8. [PubMed: 12930892]
21. Seeman P The membrane actions of anesthetics and tranquilizers. Pharmacol Rev. 1972;24(4):583–655. [PubMed: 4565956]
22. Anderson M, Omri A. The effect of different lipid components on the in vitro stability and release kinetics of liposome formulations. Drug Deliv. 2004;11(1):33–9. [PubMed: 15168789]
23. Natarajan JV, Chattopadhyay S, Ang M, Darwitan A, Foo S, Zhen M, et al. Sustained release of an anti-glaucoma drug: demonstration of efficacy of a liposomal formulation in the rabbit eye. PLoS One. 2011;6(9):e24513. [PubMed: 21931735]
24. Chen Z, Deng J, Zhao Y, Tao T. Cyclic RGD peptide-modified liposomal drug delivery system: enhanced cellular uptake in vitro and improved pharmacokinetics in rats. Int J Nanomedicine. 2012;7:3803–11. [PubMed: 22888235]
25. Sur S, Fries AC, Kinzler KW, Zhou S, Vogelstein B. Remote loading of preencapsulated drugs into stealth liposomes. Proc Natl Acad Sci U S A. 2014;111(6):2283–8. [PubMed: 24474802]
26. Fletcher CV, Staskus K, Wietgrefe SW, Rothenberger M, Reilly C, Chipman JG, et al. Persistent HIV-1 replication is associated with lower antiretroviral drug concentrations in lymphatic tissues. Proc Natl Acad Sci U S A. 2014;111(6):2307–12. [PubMed: 24469825]
27. Rossi F, Querido B, Nimmagadda M, Cocklin S, Navas-Martin S, Martin-Garcia J. The V1–V3 region of a brain-derived HIV-1 envelope glycoprotein determines macrophage tropism, low CD4 dependence, increased fusogenicity and altered sensitivity to entry inhibitors. Retrovirology. 2008;5:89. [PubMed: 18837996]
28. Parboosing R, Maguire GE, Govender P, Kruger HG. Nanotechnology and the treatment of HIV infection. Viruses. 2012;4(4):488–520. [PubMed: 22590683]
29. Stevenson M. HIV-1 pathogenesis. Nat Med. 2003;9(7):853–60. [PubMed: 12835705]
30. Desormeaux A, Bergeron MG. Lymphoid tissue targeting of anti-HIV drugs using liposomes. Methods Enzymol. 2005;391:330–51. [PubMed: 15721390]
31. Kuzmina A, Vaknin K, Gdalevsky G, Vyazmensky M, Marks RS, Taube R, et al. Functional Mimetics of the HIV-1 CCR5 Co-Receptor Displayed on the Surface of Magnetic Liposomes. PLoS One. 2015;10(12):e0144043. [PubMed: 26629902]
32. Freeling JP, Ho RJ. Anti-HIV drug particles may overcome lymphatic drug insufficiency and associated HIV persistence. Proc Natl Acad Sci U S A. 2014;111(25):E2512–3. [PubMed: 24889644]
33. Morton TA, Bennett DB, Appelbaum ER, Cusimano DM, Johanson KO, Matico RE, et al. Analysis of the interaction between human interleukin-5 and the soluble domain of its receptor using a surface plasmon resonance biosensor. J Mol Recognit. 1994;7(1):47–55. [PubMed: 7986567]
34. Jenssen H, Aspmo SI. Serum stability of peptides. Methods Mol Biol. 2008;494:177–86. [PubMed: 18726574]
35. Montefiori DC. Evaluating neutralizing antibodies against HIV, SIV, and SHIV in luciferase reporter gene assays. Curr Protoc Immunol. 2005;Chapter 12:Unit 12 1.
36. Kalyana Sundaram RV, Li H, Bailey L, Rashad AA, Aneja R, Weiss K, et al. Impact of HIV-1 Membrane Cholesterol on Cell-Independent Lytic Inactivation and Cellular Infectivity. Biochemistry. 2016;55(3):447–58. [PubMed: 26713837]

JUSTIFICATION STATEMENT

The current study demonstrates that cyclization of potent peptide based HIV-1 entry inhibitors improves their pharmacokinetic properties, and that the *in vivo* half-life is further enhanced by PEGylated liposome encapsulation, suggesting their therapeutic potential for HIV-1 infection.

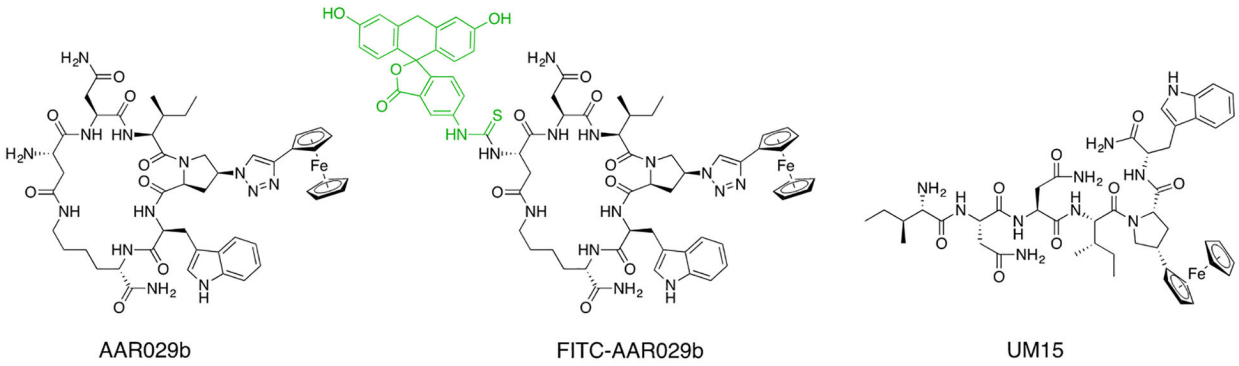

Figure 1.

Chemical structures of cPTs AAR029b and FITC-AAR029b, and of the linear hexapeptide triazole UM15.

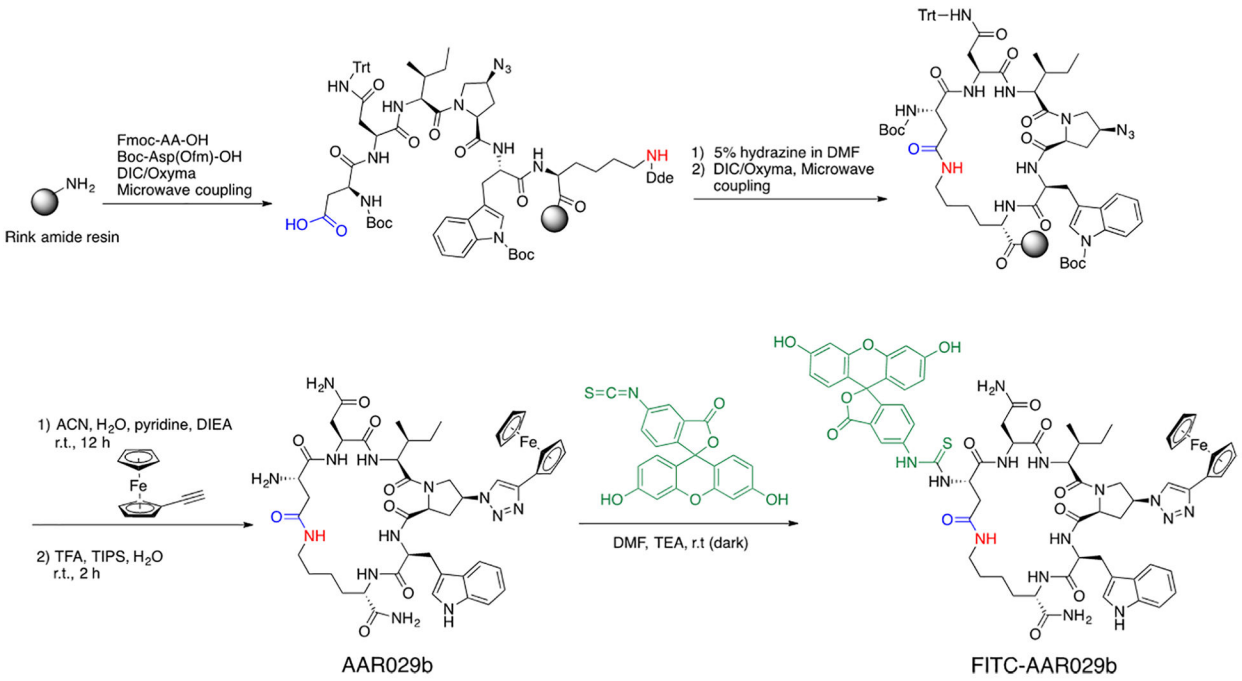

Figure 2.
Chemical synthesis of cPT AAR029b and FITC labeling

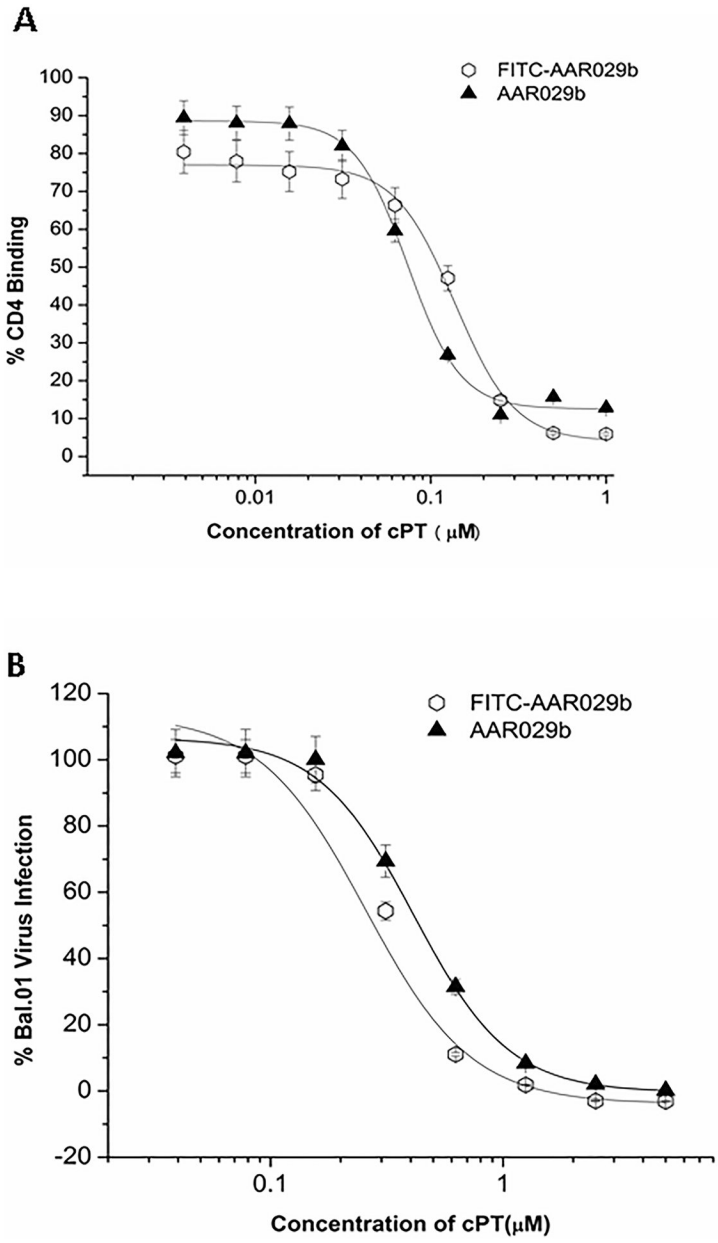

Figure 3.

Comparison of functional properties of AAR029b and FITC conjugated AAR029b. (**A**) Competition surface plasmon resonance biosensor interaction analysis. Binding of AAR029b and FITC-AAR029b to gp120 was measured by competition of wt $gp120_{YU-2}$ binding to sCD4 immobilized on CM5 sensor chip. Normalized binding response units (RUs) were measured at 5 s before the end of association. Signal obtained from exposure of sensor surface to peptide alone was subtracted, and resulting net signals were plotted *vs* peptide concentration. Fits obtained from applying a 4-parameter sigmoidal logistic equation to the data points are overlaid. (**B)** Antiviral potencies from single round cell infection assays. Recombinant HIV-1 BaL.01 virus was pre-incubated with serial dilutions of AAR029b and FITC-AAR029b for 30 min at 37 °C. The virus–inhibitor mixture was then

added to HOS.CD4.CCR5 for 48 h. Infection was determined based on luciferase activity. IC_{50} values were obtained by fitting data points to a simple sigmoidal inhibition model using the Origin software package to derive the best-fit lines. Data represent a minimum of three repeats.

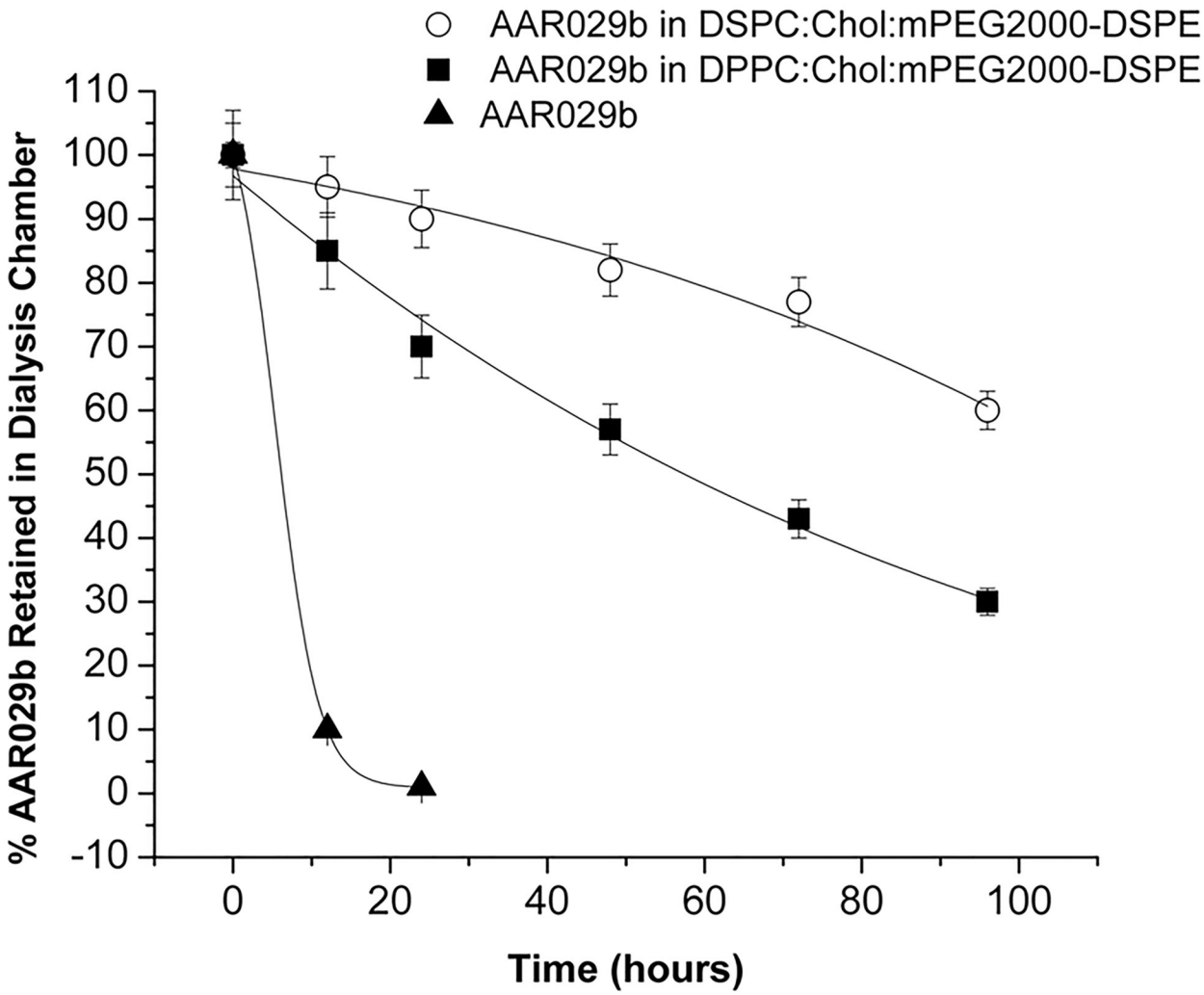

Figure 4.

In vitro release profile of free non-encapsulated AAR029b, AAR029b from DPPC:Chol:mPEG2000-DSPE liposomes, and AAR029b from DSPC:Chol:mPEG2000-DSPE liposomes at 37 °C in PBS buffer for 96 hours.

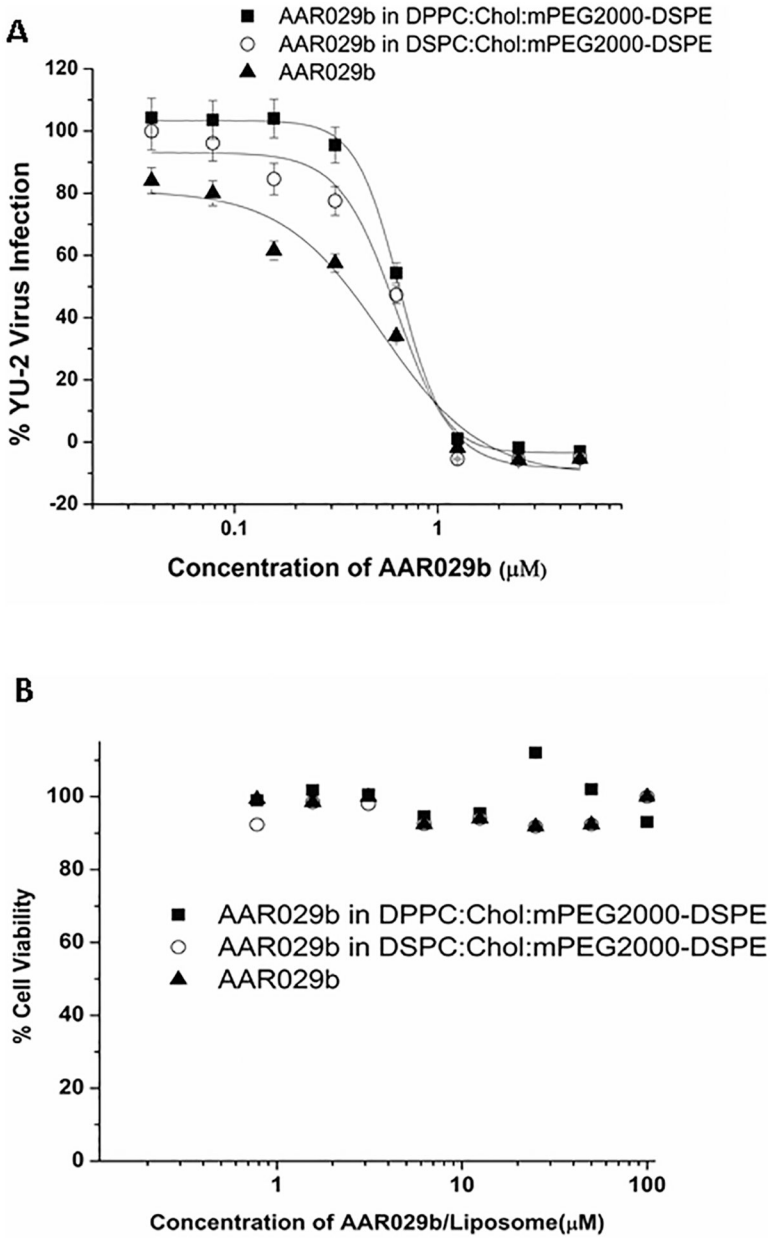

Figure 5.

(**A**) Infection inhibition efficacies of AAR029b and its liposomal formulations for lab adapted YU-2 virus and HOS.CD4.CCR5 cells, and (**B**) cell viability profile of AAR029b and its liposomal formulations with target HOS.CD4.CCR5 cells. Data are for free non-encapsulated AAR029b, AAR029b in DPPC:Chol:mPEG2000-DSPE, and AAR029b in DSPC:Chol:mPEG2000-DSPE.

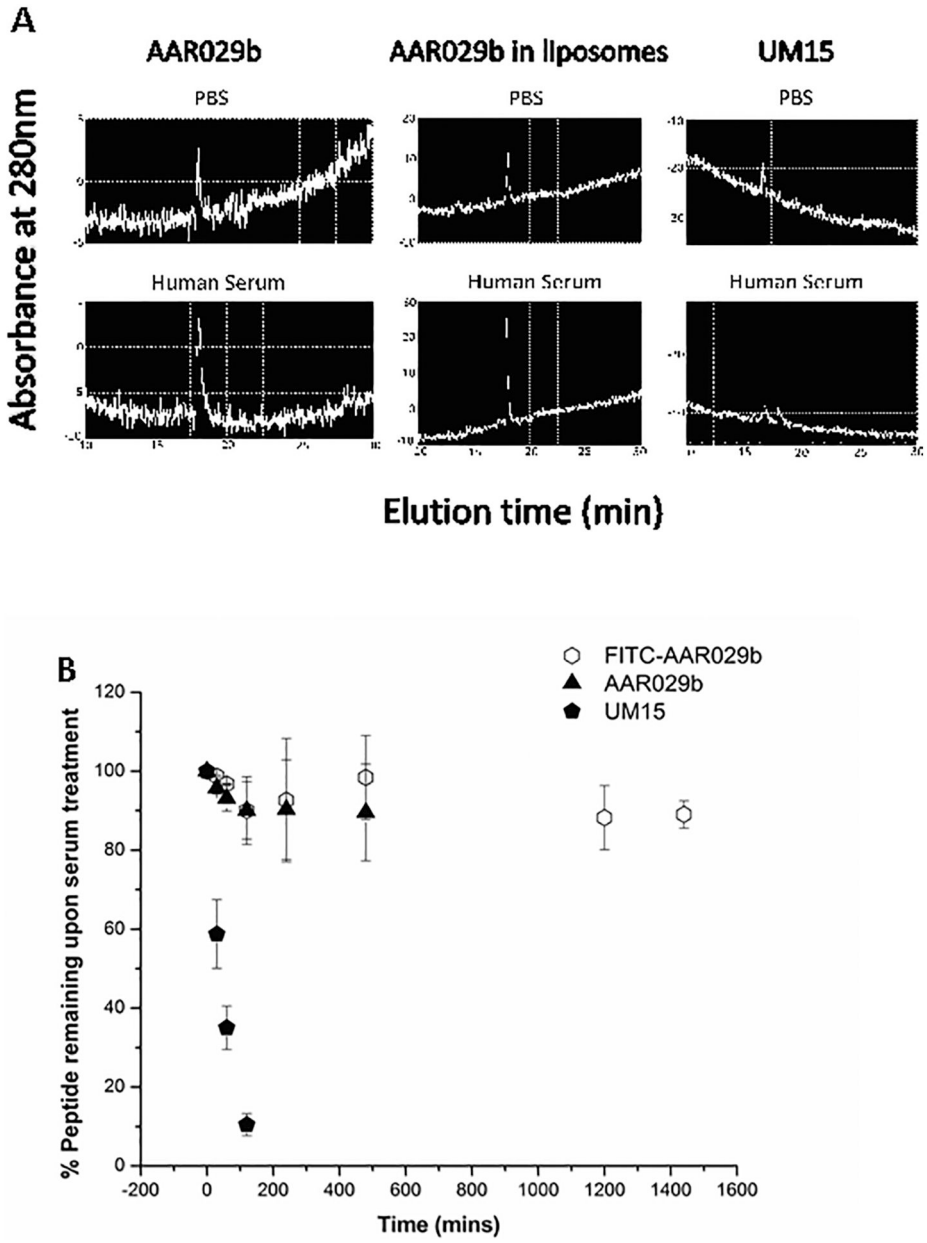

Figure 6.

A) *In vitro* serum stability profiles of UM15 (linear peptide), AAR029b and AAR029b in DSPC:Chol:mPEG2000-DSPE liposome formulation measured by UV absorbance (280 nm) of RP-HPLC chromatograms after 5 hour incubation with PBS buffer (top) and human serum (bottom) at 37 °C. **B)** The percent remaining of AAR029B, FITC-AAR029B and UM15 after treatment with serum for 24hrs calculated after normalizing with UV absorbance (at 280nm) of the samples not treated with serum protease.

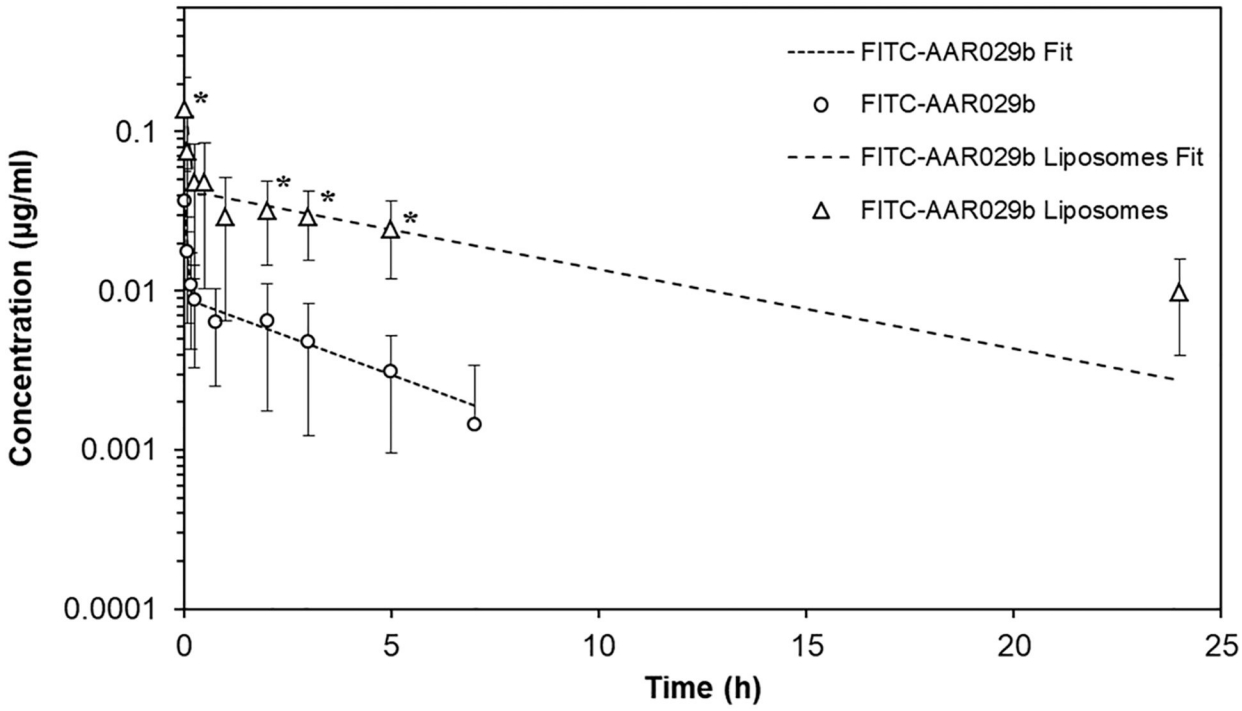

Figure 7.

In vivo circulation of FITC-AAR029b and its DSPC:Chol:mPEG2000-DSPE liposome formulation measured by fluorescence intensity of FITC-AAR029b in plasma. Pharmacokinetic profiles of FITC-AAR029b and FITC-AAR029b liposomal formulation were calculated by *PkSolver* software (40). Data are presented as mean ± SD, n = 4. * $p < 0.05$ vs. AAR029b (statistical significance was calculated using ANOVA). Dotted lines indicate the predicted fits of the experimental data points (symbols) using a two-compartment model equation.

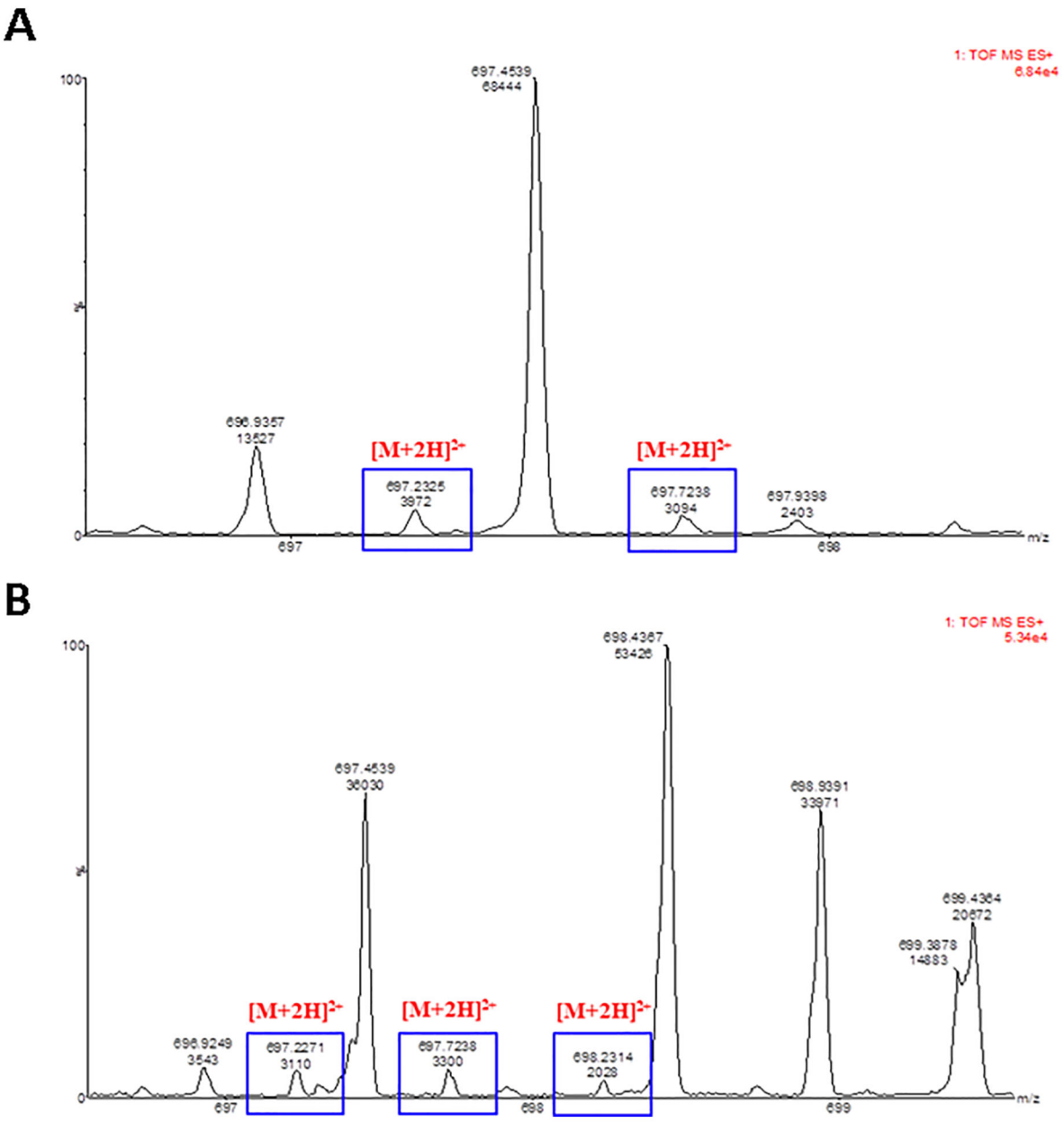

Figure 8.

UPLC chromatograms and mass spectra of plasma-derived liposomal FITC-AAR029b. A) Chromatograms overlaid with mass spectral data for the liposomal FITC-AAR029b pharmacokinetic time point at 15 min, rat#3, isotope distribution. The squares $[M+2H]^{2+}$ indicate the double charged FITC-AAR029b signal isotopic distribution; each signal differs by 0.5; B) Chromatograms overlaid with mass spectral data for the liposomal FITC-AAR029b pharmacokinetic time point at 3 h, rat#3, isotope distribution. The squares $[M+2H]^{2+}$ indicate the double charged FITC-AAR029b signal isotopic distribution; each signal differs by 0.5.

Table 1.

Inhibition efficacies of macrocyclic AAR029b and FITC-AAR029b. CD4 and 17b IC_{50} values were determined by competition SPR. Antiviral EC_{50} values were obtained by a single round cell infection assay and expressed as relative infection *versus* untreated (100%).

cPT	CD4 (IC_{50}, nM)	17b (IC_{50}, nM)	Bal.01 (EC_{50}, nM)
AAR029b	140±15	145 ±21	210 ±10
FITC-AAR029b	128±10	135 ±19	320 ±20

Table 2.

Lipid composition, diameter and encapsulation efficiency of liposome formulations containing macrocyclic peptide triazole AAR029b.

Lipid Composition	Diameter (nm)	Polydispersity Index	Encapsulation Efficiency (%)
DPPC:Chol:mPEG2000-DSPE (2:1:0.5)	163±5	0.116	51±5
DSPC:Chol:mPEG2000-DSPE (2:1:0.5)	167±5	0.129	55±4

Table 3.

Cell-based infection inhibition of macrocyclic AAR029b and its liposome formulations against HIV-1 pseudotyped Bal.01, YU-2 and JRFL viruses.

Inhibitor Composition	Bal.01 EC_{50} (nM)	YU-2 EC_{50} (nM)	JRFL EC_{50} (nM)
AAR029b	210±16	529±22	230±10
AAR029b in DPPC:Chol:mPEG2000-DSPE	215±15	649±23	256±15
AAR029b in DSPC:Chol:mPEG2000-DSPE	310±20	623±21	270±17

Table 4.

Pharmacokinetic parameters of FITC-AAR029b and its DSPC: Chol:mPEG2000-DSPE liposome formulation after intravenous bolus administration of 0.01 mg/kg FITC (equiv) to Sprague-Dawley rats. AUC, area under the curve; $t_{1/2\alpha}$, distribution half life, $t_{1/2\beta}$, elimination half life; CL, clearance; and VD, volume of distribution. Data were obtained by two repeats of the experiment.

Compound	$t_{1/2\alpha}$ (h)	$t_{1/2\beta}$ (h)	AUC 0-inf (μg h/ml)	CL (ml/h)	VD (ml)
FITC-AAR029b	0.029±0.01	2.92±0.93	0.04±0.04	136.41±30.74	541.89±118.56
FITC-AAR029b in Liposome	0.032±0.005	8.87±3.17	0.41±0.003	9.81±0.06	128.14±41.22